

ABID: Angle Based Intrinsic Dimensionality

Erik Thordsen^[0000-0003-1639-3534] and Erich Schubert^[0000-0001-9143-4880]

TU Dortmund University, Dortmund, Germany
 {erik.thordsen,erich.schubert}@tu-dortmund.de

Abstract. The intrinsic dimensionality refers to the “true” dimensionality of the data, as opposed to the dimensionality of the data representation. For example, when attributes are highly correlated, the intrinsic dimensionality can be much lower than the number of variables. Local intrinsic dimensionality refers to the observation that this property can vary for different parts of the data set; and intrinsic dimensionality can serve as a proxy for the local difficulty of the data set.

Most popular methods for estimating the local intrinsic dimensionality are based on distances, and the rate at which the distances to the nearest neighbors increase, a concept known as “expansion dimension”. In this paper we introduce an orthogonal concept, which does not use any distances: we use the distribution of angles between neighbor points. We derive the theoretical distribution of angles and use this to construct an estimator for intrinsic dimensionality.

Experimentally, we verify that this measure behaves similarly, but complementarily, to existing measures of intrinsic dimensionality. By introducing a new idea of intrinsic dimensionality to the research community, we hope to contribute to a better understanding of intrinsic dimensionality and to spur new research in this direction.

1 Introduction

Intrinsic Dimensionality (ID) estimation is the process of estimating the dimension of a manifold embedding of a given data set either at each point of the data set individually or for the entire data set at large. While describing the dimension of a given algebraic set at a specific point is a well-understood problem in algebra [21], lifting these methods to a sample of an unknown function is not trivially possible. Therefore methods that are very different from functional analysis are required to grasp the dimensionality of a discrete data set. Prior work in the field is largely focused on analyzing the differential of point counts in changing volumes [1,10,12,14], as linear algebra gives estimates of these differentials assuming a certain dimensionality. These approaches rely on distances between points and assume the data to be uniformly sampled from their defining space. The resulting ID describes the dimension required to embed a point and its neighborhood in a manifold with reasonably small loss of precision. In our novel approach for ID estimation, we derive an estimate based on the cosines between directional vectors of a point to all points in its neighborhood. The basic idea is visualized in Fig. 1: in two-dimensional dense data, we see all directions

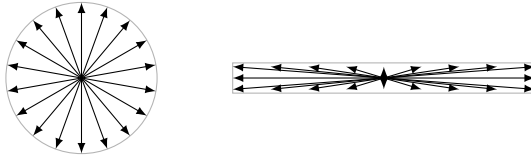


Fig. 1: Motivation of angle-based intrinsic dimensionality: in two-dimensional dense data, we see all directions evenly, in noised one-dimensional linear data arrows go either in similar or in opposite directions.

evenly, whereas in a linear subspace we mostly see parallel or opposite directions. Hence we aim at deriving an estimator capable of computing the angles between observed data points. It differs from the distance- and volume-based approaches as it describes the least dimensions required to connect a given point to the rest of the data set. It can, therefore, be understood as a description of the simplicial composition of the data set. Besides describing a different notion of local dimensionality, we provide evidence that our approach is more robust and gives stable estimates on smaller neighborhoods than the volume-based approaches. We hope that in the future the new angle-based interpretation of intrinsic dimensionality will be combined with expansion-rate-based approaches and spur further research in intrinsic dimensionality.

In Section 2 we first discuss related work. We then discuss theoretical considerations of dimensionality (and why it is not uniquely definable) in Section 3 and derive basic mathematical properties of angle distributions. In Section 4 we introduce estimation techniques using this new angle-based notion of intrinsic dimensionality, which we experimentally validate in Section 5 before we conclude the paper in Section 6.

2 Related Work

Intrinsic dimensionality has been shown to affect both the speed and accuracy of similarity search problems such as approximate nearest-neighbor search and the algorithms developed for this problem [18,4,7]. Intrinsic dimensionality has also been employed to improve the quality of embeddings [19], to detect anomalies in data sets [15], to determine relevant subspaces [6], and to improve generative adversarial networks (GANs) [5]. Distance-based estimation of intrinsic dimensionality is the “short tail” equivalent of extreme value theory [12,13], and many techniques can be adapted from estimators originally devised for extreme values on the long tail of (censored-) distributions [2], as previously used in disaster control. Important estimators include the Hill estimator [10], the aggregated version of it [16], the Generalized Expansion Dimension [14], method of moments estimators [1], regularly varying functions [1], and probability-weighted moments [1]. ELKI [20] also includes L-moments [11] based adaptations of this and improves the bias of these estimators slightly. A noteworthy recent development is the inclusion of pairwise distances as additional measurements [9] and the idea of

also taking virtual mirror images of observed data points into account [3]. We will note interesting parallels between these methods and our new approach.

Angle-based approaches have been successfully used for outlier-detection in high-dimensional data, for example with the method ABOD [17], which considers points with a low variance of the (distance-weighted) angle spectrum to be anomalous, with the assumption that such points are on the “outside” of the data set. Our approach brings ideas from this method to the estimation of intrinsic dimensionality (which in turn has been shown to relate to outlierness [15]).

3 On the Dimensionality of Functions and Data

The dimensionality of a vector field in linear algebra is the number of components of each vector; a quantity referred to as *representational dimensionality* because it characterizes the data representation more than the underlying data. By selecting components of the vectors, we can trivially obtain lower-dimensional projections. Extending this to arbitrarily oriented linear projections gives us affine subspaces also called *linear manifolds*. Yet, this is still not able to capture all varieties of dimensionality that we use: consider the map $(x) \mapsto (x, \sin x)$, which clearly is a (non-linear) embedding of a one-dimensional input space into a two-dimensional representation. Because of this smooth map, and the ability to approximate the resulting data to arbitrary precision with infinitesimal short linear pieces, we consider such a curve to be a one-dimensional manifold. This often aligns with human intuition, for example when differentiating a circle (the outline) from the corresponding disc (the contained area). Yet, the mathematical notion of manifolds also has limitations: consider the figure eight, which to a large extent resembles a line, just as the circle – except for the crossing point of the two lines, where a linear approximation is no longer possible. Similar problems will arise when we have to deal with a finite sample from the data. For example, consider many parallel lines, close to each other. Analytically, every sample will be from such a one-dimensional manifold. Yet, given only a finite set of samples and close enough lines, the resulting data resembles a two-dimensional plane.

The concept of *local intrinsic dimensionality* (LID) [12,13] captures the need for allowing different parts of a data set to have different dimensionality. Nevertheless, the “correct” answer to the question of dimensionality is all but unambiguous: in the figure eight example, the data is generated by a one-dimensional process, and also the expansion rate is linear, but at the same time the crucial point cannot be locally approximated with a one-dimensional linear function. A point on the surface of a ball (in d dimensions) of uniform density lies on the $(d-1)$ -dimensional sphere surface, while points in the interior are d -dimensional – which dimensionality should it be assigned?

In data analysis, we do not know the underlying functions. Sometimes we may aim at selecting the best match from a given set of candidate functions, but in many real problems we do not want to restrict ourselves to such a candidate set, and we may not have enough data to become reasonably confident to have found the “best” such function. Hence, we opt for a non-parametric approach

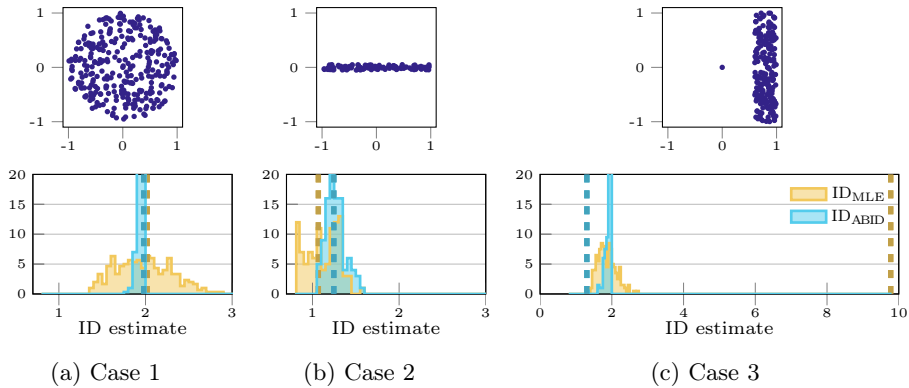


Fig. 2: Three data sets with corresponding ID estimate histograms. The dashed vertical lines correspond to the ID estimate of the point at $(0, 0)$.

instead, where we attempt to estimate the dimensionality based on the data samples; often centered around a particular point of interest.

Whilst existing work focuses on the analysis of distances in enclosing neighborhoods, our novel approach utilizes the distribution of pairwise angles of neighboring points. The different nature of the resulting ID estimates is showcased in Fig. 2. Both the distance-based (ID_{MLE} , [10]) and the angle-based (ID_{ABID} , this article) approach consider Case 2 to be dominantly one-dimensional and Cases 1 and 3 to be mostly two-dimensional. The outlying point $(0, 0)$ in Case 3, however, is judged very differently by both approaches. The distance-based approach ID_{MLE} considers its environment to be almost ten-dimensional (≈ 9.78) as all distances are very close, whereas our novel angle-based approach ID_{ABID} considers it to be one-dimensional (≈ 1.18) as the observed neighborhood lies in a narrow cone, similar to Case 2. With increased neighborhood size this cone widens and the ID gets closer to 2. This effect is similar to visual details of a surface disappearing at a distance. In the example of a point on the surface of a d -ball mentioned above, the angle-based approach is hence inclined to give an estimate below d in contrast to distance-based approaches.

We will now lay the mathematical foundations for our novel ID estimator. When estimating the ID of a given point from a data set, the general approach is to consider a number of nearby points as an enclosing neighborhood. An assumption shared by all ID estimators is that this neighborhood should be “representative” of an underlying manifold. In approaches like GED [14], “representative” can be understood as uniformly sampled from the parameter space. We hence assume that nearby points behave like a uniformly random sampled d -dimensional subspace of the embedding space, where d is the dimension of some manifold, representing the sampled parameter space. When analyzing the neighborhood of some point x , we can compute the angles between the directional vectors $x_i - x$ for all points x_i in the neighborhood of x . As the angles are independent of the lengths of these vectors, we can without loss of generality

assume that they lie on a unit sphere. We are therefore interested in the angles between points sampled uniformly random from some unit d -sphere. It is noteworthy that the unit d -sphere contains all unit d' -spheres with $d' \leq d$ as a subset. Hence, this assumption holds for any intrinsic dimensionality equal to or lower than that of the embedding space whenever the embedding is locally linear. Assuming that all vectors describing the neighborhood lie on a unit sphere, we can use the distribution of pairwise angles provided by Cai, Fan, and Jiang [8].

Theorem 1 (Distribution of random angles in a d -sphere). *The distribution of angles θ between two random points sampled independently and uniformly from a d -sphere converges, as the number of samples goes to infinity, to*

$$P(\theta) = \frac{\Gamma(\frac{d}{2})}{\Gamma(\frac{1}{2})\Gamma(\frac{d-1}{2})} \cdot \sin(\theta)^{d-2} \quad (1)$$

where Γ is the gamma function and θ is defined on $[0, \pi]$.

Proof. See Cai, Fan, and Jiang [8] for a detailed proof.

Because angles are invariant of the vector lengths, this also holds for points sampled from a d -ball instead of the sphere as well as other rotation invariant distributions such as spherical Gaussians, as long as the origin point is not included in the data (for which the angle is undefined). Note that such points at distance 0 cause problems for most estimators of intrinsic dimensionality and are commonly removed for such estimators, too.

As popularly known from the *curse of dimensionality*, all angles tend to become approximately orthogonal as dimensionality approaches infinity. This causes Eq. (1) to concentrate around $\frac{\pi}{2}$ [8]. The distribution above is unwieldy and expensive to compute (as we need to compute the arcus cosines). We, therefore, prefer to work directly on the cosines. By applying the Legendre duplication formula and doing a change of variables, we obtain the distribution of cosines.

Theorem 2 (Distribution of cosine similarities of points in a d -sphere). *The distribution of pairwise cosine similarities C between random points sampled independently and uniformly from a d -sphere is*

$$P(C) = \frac{1}{2}B(\frac{1+C}{2}, \frac{d-1}{2}, \frac{d-1}{2}) \quad (2)$$

where $B(x; \alpha, \beta)$ is the beta distribution p.d.f. and C is defined on $[-1, 1]$.

Proof. For this proof, we modify the well known Legendre duplication formula:

$$\begin{aligned} \Gamma(x)\Gamma(x + \frac{1}{2}) &= 2^{1-2x}\Gamma(\frac{1}{2})\Gamma(2x) \\ \frac{\Gamma(x + \frac{1}{2})}{\Gamma(x)\Gamma(\frac{1}{2})} &= \frac{2^{1-2x}\Gamma(2x)}{\Gamma(x)^2} = \frac{1}{B(x, x)} \cdot \frac{1}{2} \end{aligned} \quad (3)$$

where $B(\cdot, \cdot)$ is the beta function. By using this in Eq. (1) for $x = \frac{d-1}{2}$, we obtain

$$P(\theta) = \frac{1}{B(\frac{d-1}{2}, \frac{d-1}{2})} \cdot (\frac{1}{2}\sin(\theta))^{d-2}$$

We can now substitute θ with $\arccos(C)$ by a change of variable:

$$\begin{aligned}
P(C) &= \frac{1}{B(\frac{d-1}{2}, \frac{d-1}{2})} \cdot \left(\frac{1}{2} \sin(\arccos(C))\right)^{d-2} \cdot \left|\frac{\partial}{\partial C} \arccos(C)\right| \\
&= \frac{1}{B(\frac{d-1}{2}, \frac{d-1}{2})} \cdot \left(\frac{1}{2} \sqrt{1-C^2}\right)^{d-2} \cdot \frac{1}{\sqrt{1-C^2}} \\
&= \frac{1}{B(\frac{d-1}{2}, \frac{d-1}{2})} \cdot \left(\frac{(1-C)(1+C)}{2 \cdot 2}\right)^{\frac{d-2}{2}} \cdot ((1-C)(1+C))^{-\frac{1}{2}} \\
&= \frac{1}{B(\frac{d-1}{2}, \frac{d-1}{2})} \cdot \left(1 - \frac{1+C}{2}\right)^{\frac{d-1}{2}-1} \cdot \left(\frac{1+C}{2}\right)^{\frac{d-1}{2}-1} \cdot \frac{1}{2} \\
&= \frac{1}{2} B\left(\frac{1+C}{2}; \frac{d-1}{2}, \frac{d-1}{2}\right)
\end{aligned}$$

which is a beta distribution rescaled to the interval $[-1, 1]$, on which C is defined.

Based on this, we can easily obtain the following helpful corollary:

Corollary 1. *The average cosine similarity of two random points sampled independently and uniformly from a d -ball is given by*

$$\mathbb{E}[C] = 0.$$

The variance and the non-central second moment are given by

$$\text{Var}(C) = \mathbb{E}[C^2] = \frac{1}{d}.$$

Proof. This follows immediately from the central moments of beta distributions. By Theorem 2 we have $\frac{1+C}{2} \sim B(\frac{d-1}{2}, \frac{d-1}{2})$. This *symmetric* beta distribution has a mean of $\frac{1}{2}$, and hence $\mathbb{E}[C]=0$. The variance of this beta distribution given $\alpha=\beta=\frac{d-1}{2}$ is $\text{Var}(\frac{1+C}{2})=\frac{1}{4d}$, and hence $\mathbb{E}[(\frac{1+C}{2} - \frac{1}{2})^2]=\mathbb{E}[\frac{C^2}{4}]=\frac{1}{4d}$. Because the mean is 0, the variance and the second non-central moment agree trivially.

4 Estimating Intrinsic Dimensionality

Based on this theoretical distribution of cosine similarities in a d -ball, we propose new estimators of intrinsic dimensionality based on the method of moments. Similar to other estimators, we assume the data sample comes from the local neighborhood of a point; usually from a ball. The first moment of Corollary 1 cannot be used for estimation because it does not depend on d . Both the variance and the second non-central moment, however, are suitable for estimating intrinsic dimensionality, as they depend inversely on d . This simple dependency stands in contrast to the expansion-rate based approaches, which generally obtain an exponential relation to the dimensionality, as the volume of a d -ball has d in its exponent. With this simpler dependency on d , we hope to obtain a more robust measure even with smaller neighborhood sizes (fewer samples); and as we do not need to compute logarithms it can be computed more efficiently. But we still have two choices: we can either estimate using the variance $\hat{d}=1/\text{Var}(C)$ or using the non-central second moment $\hat{d}=1/\mathbb{E}[C^2]$, which only agrees if $\mathbb{E}[C]=0$ as expected for a uniform ball.

Consider the scenario of many points sampled from a hyperplane, but the point of interest is not on this hyperplane. The local neighborhood will then

consist of samples in a circular region on this plane. If we move the point of interest away from the plane, the average cosine between the samples tends to 1, and the variance to 0. The variance-based estimate would hence tend to infinity. The second non-central moment will, as the average cosine tends to 1, also tend to 1, and we estimate $d \rightarrow 1$. We argue that this is the more appropriate estimate, as the data concentrates in a single far away area.

Inspired by the work of Amsaleg et al. [3], we investigated the idea of also considering the reflections of all points with respect to the point of interest. Such a reflection would cause the average cosine in this example to be 0, as every pair of points can be matched to the pair with the second point reflected. In the above example, we would obtain two opposite discs of points and the resulting variance would tend to 1. The estimates of the variance-based estimator would thus agree with the non-central moment. We can show that when adding reflected points, the variance and the non-central second moment become equivalent (which could serve as additional justification for the approach of [3]): Since $c(x_i, -x_j) = -c(x_i, x_j) = c(-x_i, x_j)$, taking reflections into account simply means that we obtain two positive and two negative copies of each cosine. The resulting average then is always exactly 0, and hence $\text{Var}(C') = \mathbb{E}[C'^2] - \mathbb{E}[C']^2 = \mathbb{E}[C'^2] = \mathbb{E}[C^2]$. We, therefore, do not further consider using such reflections of points, besides their implicit presence in the non-central second moment.

Up to this point, we have been working with the limit cases of distributions. In the following, we now change to working with a fixed data sample of k points, centered around a point of interest. For simplicity, we assume that the data has been translated, such that the point of interest is always at the origin, and that this point (as well as any duplicates of it) has been removed from the sample. We will now work with *all pairwise* cosine similarities in a $k \times k$ matrix denoted C . The diagonal of this matrix is usually excluded from computations. We use the term C_1 when the ones on the diagonal are to be included. By C^2 , we denote the individual squaring of cosines. The next theorem will use both a fixed sample and the matrix C_1 with the diagonal included.

Theorem 3 (Upper bound). *Let $X = \{x_1, \dots, x_k\} \subset \mathbb{R}^D$ be a sample from a d -dimensional subspace embedded in \mathbb{R}^D for some $d \leq D$. Formally, let X contain at least d linearly independent vectors and let all x_i be linear combinations of a given set of d orthonormal basis vectors. Then the following inequality holds*

$$\mathbb{E}[C_1^2]^{-1} \leq d.$$

Proof. Let \tilde{X} be the $k \times d$ matrix obtained from X by first performing a change of basis to the given orthonormal basis of size d , then normalizing each vector to unit length to produce \tilde{x}_i . Neither the change of basis (which is a rotation) nor the posterior normalization affects the cosine similarities, and we hence have

$$c(\tilde{x}_i, \tilde{x}_j) = c(x_i, x_j). \tag{4}$$

It immediately follows that \tilde{X} has a rank of d , as we still have d linearly independent vectors. The matrix $\tilde{C}_1 = \tilde{X}\tilde{X}^T$ then contains entries of the form $\langle \tilde{x}_i, \tilde{x}_j \rangle$.

As all \tilde{x}_i are normalized, \tilde{C}_1 is equal to the cosine similarities. Per Eq. (4) it then follows that \tilde{C}_1 is exactly C_1 . Because C_1 is a cosine similarity matrix, the diagonal entries are all 1, and we have $\text{tr}(C_1)=k$. Since \tilde{X} is a $k \times d$ matrix with rank d , we know that the rank of C_1 is d as well. Therefore C_1 has d eigenvalues $\lambda_1, \dots, \lambda_d$ with $\sum_{i=1}^d \lambda_i = \text{tr}(C_1) = k$. The sum of squared entries $\|C_1\|_2^2$ equals the sum of squared eigenvalues $\sum_{i=1}^d \lambda_i^2$ and is minimized if every eigenvalue equals $\frac{k}{d}$, which means we have the following lower bound:

$$\|C_1\|_2^2 = \sum_{i=1}^d \lambda_i^2 \geq d \cdot \left(\frac{k}{d}\right)^2 = \frac{k^2}{d} \quad (5)$$

and by taking the inverse we obtain the upper bound $\mathbb{E}[C_1^2]^{-1} \leq d$.

This is an upper bound for estimating the intrinsic dimensionality using C_1 , and we can use this to also obtain an upper bound for C .

Corollary 2. *Let $X = \{x_1, \dots, x_k\} \subset \mathbb{R}^D$ be a sample from a d -dimensional subspace embedded in \mathbb{R}^D as defined in Theorem 3. If $k > d$, then*

$$\mathbb{E}[C^2]^{-1} \leq \frac{k-1}{k-d} \cdot d. \quad (6)$$

Proof. Because the difference between C and C_1 is the diagonal of ones, Eq. (5) yields

$$\|C\|_2^2 = \|C_1\|_2^2 - k \geq \frac{k^2}{d} - k = \frac{k(k-d)}{d}$$

and hence the average of the remaining $k^2 - k$ cells is

$$\mathbb{E}[C^2] \geq \frac{k-d}{k-1} \cdot \frac{1}{d}$$

which is equivalent to the inequality above. For $k=d$ we obtain a trivial bound.

The difference of including the diagonal or not vanishes for large enough k . One could attempt to regularize $\mathbb{E}[C^2]$ with $\frac{k-1}{k-d}$. The major problem therein is that we do not know d in advance. To control the maximal overestimation of d , a sufficiently large neighborhood can be used to lower the margin of error. For example, to bound $\mathbb{E}[C^2]^{-1} \leq d+c$, at least $k \geq \frac{1}{c}d^2 + (1-\frac{1}{c})d$ neighbors are required. For the bound $d+1$ ($c=1$), this means we require $k \geq d^2$ samples.

To solve this self-referential problem, we can also attempt an iterative refinement. It turns out that the fixed point of this regularization yields exactly the result we obtain by using C_1 instead of C . Because using C_1 corresponds to using a regularized version and because it has a very elegant upper bound, we base our method on this estimate:

Definition 1 (ABID). *Given a data set $X = \{x_1, \dots, x_n\} \subset \mathbb{R}^D$, the regularized angle-based intrinsic dimensionality estimator for a point x_i is:*

$$ID_{ABID}(x_i; k) := \mathbb{E}[C_1(B_k(x_i))^2]^{-1}$$

where $B_k(x_i)$ are the directional vectors from x_i to the k nearest neighbors of x_i and $C_1(B_k(x_i))$ are the pairwise cosine similarities within $B_k(x_i)$.

By choosing the neighborhood of any point in the specified set by the k nearest neighbors, the measure is invariant under scaling. Analogously, one can instead define the neighborhood by a maximum distance to the central point. The sole restriction thereby is that the size of the neighborhood has to be greater or equal to $d+2$ as for any smaller neighborhood, the estimator does not need to be properly regularized. Since the error of the non-regularized estimate is limited for any neighborhood with size quadratic in the intrinsic dimension, we further introduce a non-regularized version for comparative analysis.

Definition 2 (RABID). *Given a data set $X = \{x_1, \dots, x_n\} \subset \mathbb{R}^D$, the raw angle-based intrinsic dimensionality estimator for a point x_i is defined as*

$$ID_{RABID}(x_i; k) := \mathbb{E}[C(B_k(x_i))^2]^{-1}$$

where $B_k(x_i)$ are the directional vectors from x_i to the k nearest neighbors of x_i and $C(B_k(x_i))$ are the pairwise cosine similarities of different vectors in $B_k(x_i)$.

Beware that this estimator can cause a division by zero if all k vectors are pairwise orthogonal, and can return values larger than k . In such cases, it is recommended to treat the estimate as k , because the input vectors span a k dimensional subspace. Nevertheless, this estimator is likely unstable for small k , and for large k , it converges to ID_{ABID} .

To interpret the estimates by the new method, it is important to consider the domain they operate on. The angle-based measure is bounded by the spanning dimensionality of the point set. While distributions of angles are usually distorted by non-linear transformations, many transformations such as rotations will retain this bound. Hence the bound may nevertheless apply—at least approximately—for many projections of lower-dimensional manifolds in higher dimensional embeddings. It is easy to see that angle-preserving transformations do not affect our measure, while distance-preserving transformations will not affect distance-based estimators. Our new measure is less affected by local non-linear contractions and expansions such as the decreasing density on the outer parts of Gaussian distributions, but it tends to estimate higher dimensionality than distance-based-approaches when the transformations are non-linear. We do not consider this to be a flaw, just a different design that may or may not have advantages: a common assumption in many methods and applications like manifold learning is to have locally linear transformations that preserve small neighborhoods, which will then affect neither angles nor densities. Our estimator, which can be seen as estimating how many dimensions such a locally linear embedding needs to have, is arguably very close to the idea of such applications.

5 Evaluation

In our comparative evaluation, we consider several ID estimators on many standard evaluation data sets of both artificial and natural origin. As measures of quality, we analyze the estimated ID’s consistency both with expected values

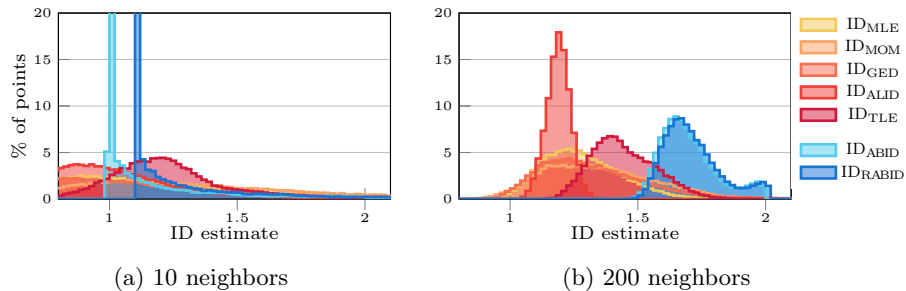


Fig. 3: Histograms of ID estimates of points sampled from a Koch snowflake.

(for synthetic data) and with each other (for natural data with no true value). We will further inspect the stability of ID estimates for varying neighborhood sizes. Depending on the density of data sets, approaches that require a large neighborhood to stabilize, tend to be inapplicable.

The histograms shown in this section are limited to a region of interest in both x and y direction for interpretability. Outside of the presented range along the x -axis, the distributions always show a smooth drop to zero with no further peaks but may have a long tail.

5.1 Reference Estimators

We compare ID_{ABID} and ID_{RABID} to the Hill estimator ID_{MLE} [10], the measure-of-moments-based estimator ID_{MOM} [1], the generalized expansion dimension ID_{GED} [14], the augmented local ID estimator ID_{ALID} [9] and its successor, the tight LID estimator ID_{TLE} [3] using the implementations in the ELKI framework [20]. All of these alternative estimators are based on the expansion rate. The ID_{TLE} is supposed to reduce the necessary sample size in the neighborhood to acquire a good estimate, yet in our experiments tends to give higher estimates than the other distance-based approaches.

5.2 Dimensionality of Fractal Curves

In line with the theoretical foundation of this work and to demonstrate the different semantics of angle-based and distance-based ID estimation, we analyze the estimated ID of a well-known fractal, the Koch snowflake. As seen in Fig. 3, most distance-based approaches estimate a dimensionality roughly around $\frac{\log 4}{\log 3} \approx 1.26$, which is the Hausdorff dimension of the Koch snowflake, when we consider enough neighbors ($k=200$). This result is not surprising, as the distance-based approaches are conceptually closely related to classical fractal dimensions. Our angle-based estimates, however, estimate a dimensionality of ≈ 1.6 for larger neighborhoods, which is larger than the fractal dimension, yet smaller than the representation dimension. The difference can be explained by the highly non-linear shape of the snowflake, as two consecutive line segments are overlapping

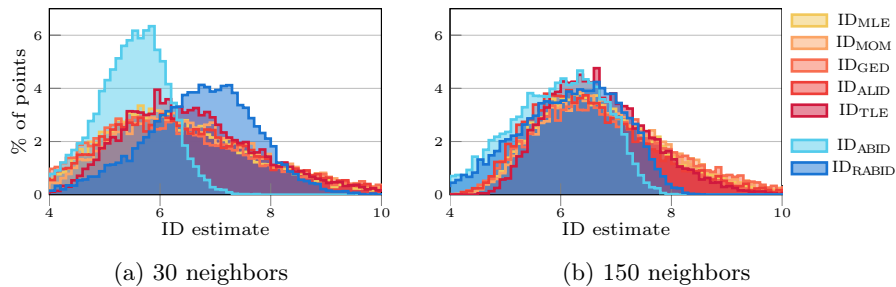


Fig. 4: Histograms of ID estimates of the `m6` set with different neighborhood sizes.

in a singularity. Because the points are sampled from a Koch snowflake with finite recursion depth, they must lie on this non-linear curve. Reproducing the exact curve from a finite sampling, however, is highly unlikely as specific parts of the embedding space, that is \mathbb{R}^2 , can be approximated to almost arbitrary precision. The dimensionality of the sampling can, therefore, be locally indistinguishable from the embedding space. Where the distance-based approaches try to estimate the minimum dimensionality that can possibly explain a model, the angle-based approaches estimate the minimum dimensionality from which a model is indistinguishable. A higher estimate as parameter choice for downstream applications, such as manifold learning, may turn out to be more robust. The results on further fractals, such as the outline of n -flakes, were similar.

It is noteworthy that the scale of the neighborhood has a large impact on the estimates. When choosing a neighborhood small enough to mostly stay within a line segment of the fractals (here $k=10$), the ID estimates approximate 1, as small neighborhoods lie on straight lines. For larger neighborhoods, the estimates approach a proper representation of the manifold space. For too large neighborhoods, however, boundaries of the point set as well as observing points distant on the manifold, yet close in the embedding space, tend to corrupt the estimates.

5.3 Synthetic Data

Amsaleg et al. [3] used a collection of synthetic and natural data sets, which they provide for download. The `m6` data set consists of points sampled from a 6-dimensional manifold non-linearly embedded in a 36-dimensional space. As can be seen in Fig. 4, for $k=150$ all estimators agree on the data set to be inherently 6-dimensional at most points. Where distance-based estimators tend to have a long tail towards higher dimensions, the angle-based approaches have an upper bound. The estimates larger than 6 therefore must be artifacts from the nonlinearity of the embedding used in this data set. Even though this nonlinearity shifts the upper bound beyond 6, the angle-based approaches tend to have a shorter upper tail and drop off faster to zero. It is noteworthy that when comparing the estimates of the same method at different neighborhood sizes between 30 and 300, the angle-based approaches achieve higher scores than

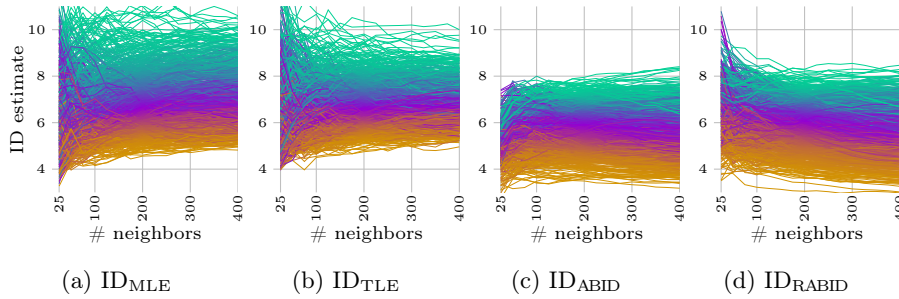


Fig. 5: Trails of estimates of 1000 points for varying neighborhood sizes on the m6 set. Trail colors are assigned in order of ID estimates at 200 neighbors.

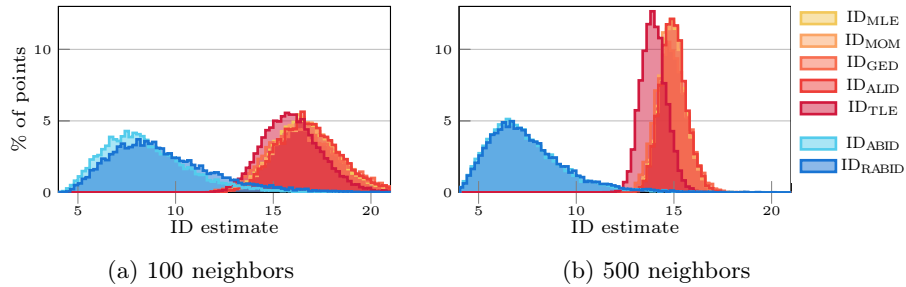


Fig. 6: Histograms of ID estimates of the m10c data set.

the distance-based approaches on both Spearman’s and Pearson’s correlation coefficients. In this sense, the angle-based approaches are more stable both in the value of the estimates as well as the order of points by estimated value when varying neighborhood sizes. In more extreme neighborhoods (<30 and >300), artifacts from having too few samples for a reliable estimate and reaching the boundaries of the data set, respectively, cause results to become less stable. The stability is visualized in Fig. 5 using trails of ID estimates for individual points when varying the neighborhood size. In a perfectly stable result, all lines would be parallel; instability causes lines that cross outside their own color range (which represents the order at $k=200$) and hence the mixing of the colors. The improved stability of the angle-based estimates is shown by a fairly stable plot from 125 to 300 neighbors, whereas the distance-based estimates begin to deviate much more at ≤ 150 and ≥ 250 neighbors respectively already. Additionally, we can see in this plot that the average (the purple region) of the distance-based estimates tends to increase with growing neighborhood size whereas the distribution of ID_{ABID} appears stable upwards of 100 neighbors. We can observe the upper bound property of ID_{ABID} compared to ID_{RABID} . The higher stability means that smaller neighborhoods suffice for proper estimates and that the neighborhood parameter is easier to choose.

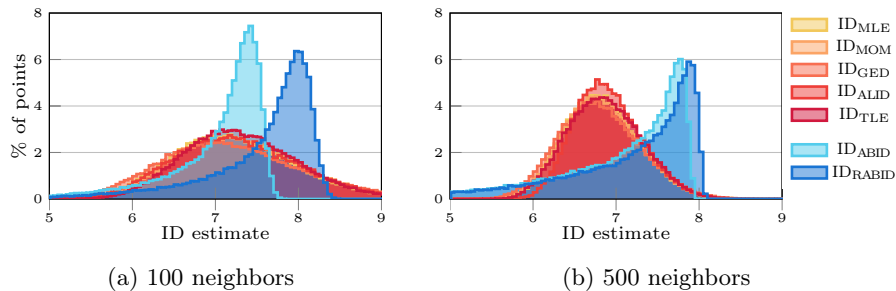


Fig. 7: Histograms of ID estimates of points on an 8-dimensional noisy lattice.

The highest intrinsic dimensional data set provided by Amsaleg et al. [3], `m10c`, is a 24-dimensional uniformly sampled hypercube embedded in 25 dimensions. On that data set, we observed a larger discrepancy between the angle- and the distance-based approaches, shown in Fig. 6. However, `m10c` consists of only 10,000 points, which is the number of corners of a $\log_2(10,000) \approx 13$ dimensional hypercube. Hence, we doubt that this small sample can reliably represent a full 24-dimensional manifold, but the data likely is of much lower dimensionality. The estimates of the distance-based approaches move towards this value as the neighborhood size increases. Each of these 10,000 points then is, however, essentially the corner of a 13-dimensional hypercube; and will see the other data points as forming a hypercone, producing smaller angles than if the data would evenly surround the point. We believe it is because of this effect (essentially a variant of the curse of dimensionality) that the angle-based approaches estimate a far lower ID. To support this theory, we created a data set consisting of points on the crossings of an 8-dimensional lattice, where each dimension is sampled at the values $0, \frac{1}{3}, \frac{2}{3},$ and 1 resulting in $4^8 = 65535$ points. To smoothen the data we added jitter to each point, uniformly drawn from $[0, \frac{1}{3}]^d$. In that way, we obtained a data set that is more evenly distributed than uniform random sampling and truly spans an 8-dimensional space. On this data set, only the angle-based approaches were able to estimate the correct dimension for most points as can be seen in Fig. 7. The many points where ID_{ABID} and ID_{RABID} estimate lower values are likely the many points at the corners, edges, and sides of this lattice.

To test the reliability of estimators in a mixture of manifolds, we created instances of 1- through 5-dimensional hypercubes linearly projected into the same 5-hypercube. The projection was chosen such that every d_i -dimensional hypercube intersects every d_j -dimensional hypercube in a $\min(d_i, d_j)$ -dimensional subspace. For every hypercube, we sampled 5000 points uniformly at random and computed ID estimates using a neighborhood of different sizes. In all experiments, the angle-based approaches were visibly more capable of differentiating between the different dimensional subspaces, which can be seen from the sharper spikes in Fig. 8. Being capable of separating lower-dimensional subspaces is an important feat, as noise in the embedding space can be considered a high-

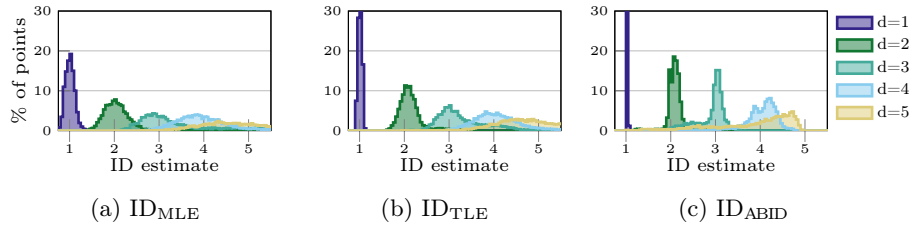


Fig. 8: Histograms of ID estimates of nested hypercubes with a neighborhood size of 100 colored by the hypercube from which they were sampled.

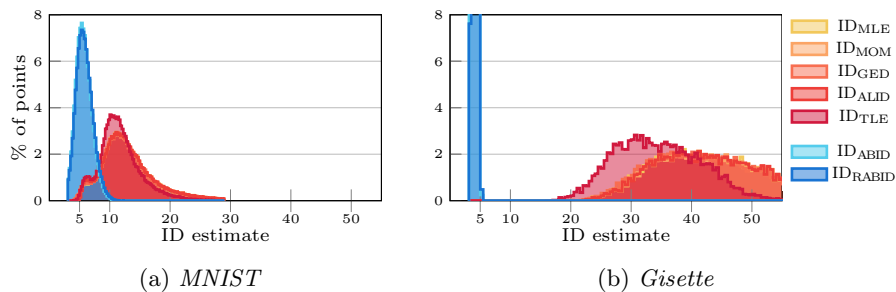


Fig. 9: Histograms of ID estimates of the entire *MNIST* data set and its noised subset *Gisette*, both with a neighborhood size of 300.

dimensional manifold containing the manifold of interest, and we believe this new ID estimate may help subspace discovery approaches that, based on intrinsic dimensionality (e.g., [6]). We observe that the angle-based approaches are more robust against noise and in the presence of overlapping subspaces.

5.4 Real Data

We also analyzed the ID estimates on natural data sets. The most interesting results were achieved on the *MNIST* data set consisting of gray-scale images of hand-written digits with a 28×28 resolution. Our proposed approach estimates an ID of about 6 for most points, whereas the distance-based approaches peak around 10 to 11. From neighborhood sizes of 100 upwards, the distance-based approaches, however, start forming a second peak at the same ID as the angle-based approaches, visible in Fig. 9. A possible explanation could be that the *MNIST* data set is not uniformly random on the manifold, whereby small environments are too noisy for distance-based approaches. That claim is further supported by a higher resolution subset of *MNIST*, *Gisette*, consisting only of handwritten 4s and 9s with a 50×50 resolution. The 2500-dimensional image vectors in *Gisette* were further expanded by just as many uniformly random dimensions, mimicking high-dimensional noise in a 5000-dimensional embedding. The added noise harshly increased the estimates of the distance-based approaches.

The angle-based approaches, however, estimate a slightly lower ID of about 4 for most points. When considering a subset of points, the ID might vary in both directions. When retaining only a surface of a hypercube, the ID should clearly reduce. When sparsening the data such that, e.g., a space-filling curve is reduced to a lattice-like data set, the ID estimate can also increase. However, we consider the smaller difference of the angle-based estimates as more plausible, even though the proposed estimates for the *Gisette* data set might be slightly too low as the high-dimensional noise might have sparsened the local neighborhoods too much. Nevertheless, we observe that the angle-based approach can be more robust against noise in such a semi-real scenario.

5.5 Estimator Interactions

These experiments can also give some insight into the differences and interactions of the different estimators. As expected from theory, ID_{ABID} and ID_{RABID} converge towards the same value for sufficiently large neighborhood sizes. Because it is trivial to compute both estimators at once, we can use the difference of the estimates to assess the quality; if they differ much we may need larger sample sizes, if they are close the sample size should be sufficient for this dimensionality. Because the angle-based estimators appear to require fewer samples than the distance-based approaches, this may also help to choose parameters for these methods. Secondly, if the angle-based estimates are much smaller than the distance-based estimates, the data set might not be sufficiently densely sampled for this dimensionality; if the angle-based estimates are much larger than the distance-based estimates, the embedding may be highly non-linear (as in the Koch snowflake example), or may not preserve local density.

6 Conclusions

In this paper, we propose a novel approach to estimate local intrinsic dimensionality, along with two estimators, ID_{ABID} and ID_{RABID} . Instead of analyzing the expansion rate, as previous distance-based approaches do, the novel approach focuses on the geometry characterized by pairwise angles. We have given an a priori derivation of the novel estimators derived from integral geometry. Our experimental evaluation suggests that the novel approach may be more robust against noise, computes a bit stabler estimates, and gives estimates as reasonable as distance-based estimators, albeit of a different nature. We have further discussed how the difference between estimates can hint at particular effects in the data. The presented approach does not yet fully utilize all interactions of the pairwise angles within a neighborhood, which could lead to an improved ID estimation in future work by incorporating ideas of [3]. Future work may also investigate using higher-order moments, as well as robust estimation techniques for the second moment, such as the median average deviation or L-moments [11]. As $E[C] \gg 0$ indicates points remote from their neighbors, this can be interesting to integrate into an outlier detection method based on intrinsic dimensionality, which would yield a hybrid of ABOD [17] and LID outlier detection [15].

References

1. Amsaleg, L., Chelly, O., Furon, T., Girard, S., Houle, M.E., Kawarabayashi, K., Nett, M.: Estimating local intrinsic dimensionality. In: KDD (2015)
2. Amsaleg, L., Chelly, O., Furon, T., Girard, S., Houle, M.E., Kawarabayashi, K., Nett, M.: Extreme-value-theoretic estimation of local intrinsic dimensionality. *Data Min. Knowl. Discov.* **32**(6) (2018)
3. Amsaleg, L., Chelly, O., Houle, M.E., Kawarabayashi, K., Radovanovic, M., Treeratanajaru, W.: Intrinsic dimensionality estimation within tight localities. In: SDM (2019)
4. Aumüller, M., Ceccarello, M.: The role of local intrinsic dimensionality in benchmarking nearest neighbor search. In: SISAP (2019)
5. Barua, S., Ma, X., Erfani, S.M., Houle, M.E., Bailey, J.: Quality evaluation of GANs using cross local intrinsic dimensionality. CoRR **abs/1905.00643** (2019)
6. Becker, R., Hafnaoui, I., Houle, M.E., Li, P., Zimek, A.: Subspace determination through local intrinsic dimensional decomposition. In: SISAP (2019)
7. Bratic, B., Houle, M.E., Kurbalija, V., Oria, V., Radovanovic, M.: The influence of hubness on NN-descent. *Int. J. Artif. Intell. Tools* **28**(6) (2019)
8. Cai, T.T., Fan, J., Jiang, T.: Distributions of angles in random packing on spheres. *J. Mach. Learn. Res.* **14**(1) (2013)
9. Chelly, O., Houle, M.E., Kawarabayashi, K.: Enhanced estimation of local intrinsic dimensionality using auxiliary distances. Tech. Rep. NII-2016-007E, National Institute of Informatics (2016)
10. Hill, B.M.: A simple general approach to inference about the tail of a distribution. *The Annals of Statistics* **3**(5) (1975)
11. Hosking, J.R.M.: L-moments: Analysis and estimation of distributions using linear combinations of order statistics. *J. Royal Stat. Soc. B* **52**(1) (1990)
12. Houle, M.E.: Local intrinsic dimensionality I: an extreme-value-theoretic foundation for similarity applications. In: SISAP (2017)
13. Houle, M.E.: Local intrinsic dimensionality II: multivariate analysis and distributional support. In: SISAP (2017)
14. Houle, M.E., Kashima, H., Nett, M.: Generalized expansion dimension. In: ICDM Workshops (2012)
15. Houle, M.E., Schubert, E., Zimek, A.: On the correlation between local intrinsic dimensionality and outlieriness. In: SISAP (2018)
16. Huisman, R., Koedijk, K.G., Kool, C.J.M., Palm, F.: Tail-index estimates in small samples. *Journal of Business & Economic Statistics* **19**(2) (2001)
17. Kriegel, H., Schubert, M., Zimek, A.: Angle-based outlier detection in high-dimensional data. In: KDD (2008)
18. Radovanovic, M., Nanopoulos, A., Ivanovic, M.: Hubs in space: Popular nearest neighbors in high-dimensional data. *J. Mach. Learn. Res.* **11**, 2487–2531 (2010)
19. Schubert, E., Gertz, M.: Intrinsic t-stochastic neighbor embedding for visualization and outlier detection - A remedy against the curse of dimensionality? In: SISAP (2017)
20. Schubert, E., Zimek, A.: ELKI: A large open-source library for data analysis - ELKI release 0.7.5 "heidelberg". CoRR **abs/1902.03616** (2019)
21. Watanabe, S.: Algebraic geometry and statistical learning theory, vol. 25. Cambridge University Press (2009)